Title

Contrast-enhanced MR Angiography without Gadolinium-based Contrast Material: Clinical Applications Using Ferumoxytol

Journal

Radiology Cardiothoracic Imaging, 4(4)

ISSN

2638-6135

Authors

Jalili, Mohammad H
Yu, Tiffany
Hassani, Cameron
et al.

Publication Date

2022-08-01

DOI

10.1148/ryct.210323

Peer reviewed

Radiology: Cardiothoracic Imaging

IMAGING ESSAY

Contrast-enhanced MR Angiography without Gadolinium-based Contrast Material: Clinical Applications Using Ferumoxytol

Mohammad H. Jalili, MD • Tiffany Yu, MD* • Cameron Hassani, MD • Ashley E. Prosper, MD • J. Paul Finn, MD • Arash Bedayat, MD*

From the Department of Radiological Sciences, David Geffen School of Medicine at UCLA, 10945 Le Conte Ave, Suite 3371, Los Angeles, CA 90095. Received January 3, 2022; revision requested February 15; revision received July 1; accepted July 15. **Address correspondence to** A.B. (email: *ABedayat@mednet.UCLA.edu*).

* M.H.J. and T.Y. contributed equally to this work.

Authors declared no funding for this work.

Conflicts of interest are listed at the end of this article.

Radiology: Cardiothoracic Imaging 2022; 4(4):e210323 • https://doi.org/10.1148/ryct.210323 • Content codes: VA MR

Vascular imaging can be challenging because of the wide variability of contrast dynamics in different vascular territories and potential safety concerns in patients with renal insufficiency or allergies. Off-label diagnostic use of ferumoxytol, a superparamagnetic iron nanoparticle approved for therapy, is a promising alternative to gadolinium-based contrast agents for MR angiography (MRA). Ferumoxytol has exhibited a reassuring safety profile when used within the dose range recommended for diagnostic imaging. Because of its prolonged and stable intravascular residence, ferumoxytol can be used in its steady-state distribution for a wide variety of imaging indications, including some where conventional MRA is unreliable. In this article, authors discuss some of the major vascular applications of ferumoxytol and highlight how it may be used to provide highly diagnostic images and improve the quality, workflow, and reliability of vascular imaging.

Contrast-enhanced MRI has a wide spectrum of applications for vascular evaluation. For more than 30 years, gadolinium-based contrast agents (GBCAs) have dominated the landscape for soft tissue and vascular enhancement. However, concerns about gadolinium deposition in brain and bone, or nephrogenic systemic fibrosis in patients with chronic kidney disease, have highlighted the need for alternative options (1–6). Noncontrast MR angiography (MRA) techniques have made substantial progress in recent years, particularly for imaging of the lower extremities. However, for many applications in the thorax and abdomen, noncontrast techniques have proved less practical and reliable than their contrast-enhanced counterparts. Also, all noncontrast MRA techniques are flow dependent, and the user is often faced with many choices regarding imaging parameters and magnetization preparation prepulses. This is further confounded by the diversity of techniques offered by different vendors and MRI platforms. In addition, in body regions sensitive to off-resonance artifacts, such as the lungs where air flows through the respiratory tracts close to the pulmonary vasculature, noncontrast MRA may be challenging (7).

Ferumoxytol was initially designed as a blood pool MRI contrast agent, but it was repurposed to the iron therapy market early in its development. In 2009, it was approved by the U.S. Food and Drug Administration (FDA) for treatment of iron deficiency in patients with chronic kidney disease (8,9). In 2012, Sigovan et al used ferumoxytol to image dialysis fistulas, highlighting its potential as an alternative to the GBCA in patients with renal disease (10). Since then, ferumoxytol has been increasingly used off-label for MRA (11,12). Additional imaging applications have included evaluation of brain tumors, organ ischemia, pathologic inflammation, and nodal metastases (13–16). In recent years, the safety of ferumoxytol for use in pediatric populations has been assessed across many studies for evaluation of lymph nodes, intracranial arteriovenous malformations, and congenital heart disease (CHD). All of these pediatric studies report high efficacy without substantial adverse effects (17–19). The only absolute contraindications to ferumoxytol are in patients with iron allergy or iron storage diseases such as hemochromatosis (9).

Because of the absence of formal FDA approval for use of ferumoxytol in diagnostic imaging, it is important for practicing radiologists and trainees to recognize how and when ferumoxytol can be used safely and effectively as an alternative or complementary contrast agent. Here, we review the vascular applications of ferumoxytol-enhanced MRA, including its benefits over GBCA-enhanced MRA and iodinated contrast-enhanced CT angiography (CTA).

Properties

Ferumoxytol is an ultrasmall superparamagnetic iron oxide with a polysaccharide coat and a mean particle size of 30 nm (20). Once infused, it has an intravascular half-life of about 15 hours in adults. Ferumoxytol is cleared from the blood by macrophages and stored in the physiologic iron pools of the body (ie, liver, spleen, bone marrow, and lymph nodes), later to be mobilized for hematopoiesis and essential intracellular metabolism (8,21,22).

The usual dose range of ferumoxytol for imaging is 3–5 mg/kg of elemental iron up to a maximum of 500 mg (23), corresponding to about half the therapy dose. In compliance with the updated 2015 FDA guidelines, ferumoxytol

Abbreviations

CHD = congenital heart disease, CTA = CT angiography, FDA = U.S. Food and Drug Administration, GBCA = gadolinium-based contrast agent, MRA = MR angiography, TAPVR = total anomalous pulmonary venous return

Summary

Ferumoxytol, a high-relaxivity, iron-based contrast agent for vascular MRI, yields high-quality thoracoabdominal images without the need for bolus timing, and its stable concentration in the blood broadens the scope of imaging applications.

Key Points

- Ferumoxytol was originally designed as a blood pool MRI contrast agent but was redirected to the therapy market as an intravenous agent to treat iron deficiency anemia, for which it is currently approved by the U.S. Food and Drug Administration.
- Ferumoxytol is a true theranostic agent, but its diagnostic use is off-label; nonetheless, it is being successfully used for MR angiography in patients with renal insufficiency or when iodinated- or gadolinium-based contrast agents are contraindicated.
- Ferumoxytol is a superparamagnetic iron oxide nanoparticle with an intravascular half-life of 15 hours; it is metabolized through the reticuloendothelial system and incorporated into the body's iron stores to support essential metabolic functions.
- The prolonged intravascular residence time of ferumoxytol facilitates high-quality imaging of complex arterial and venous anatomy and congenital heart diseases without the need for bolus timing and can also be used for imaging of stress-induced changes in vascular caliber.

Keywords

MR Angiography, MRI Contrast Agent, Cardiac, Vascular

is administered by slow infusion by trained personnel, with patient monitoring for at least 30 minutes after injection. The FDA recommends a 15-minute infusion time for the 500-mg therapy dose, which corresponds to 7–8 minutes for an average adult diagnostic dose. As a practical point, radiologists interpreting MR images of patients who recently received ferumoxytol for therapy should keep in mind that the contrast enhancement may persist for a week in brain lesions and for several weeks in liver, spleen, and bone marrow on T2-weighted images (9).

A key property of ferumoxytol is that once infused, its concentration in the blood remains essentially constant for several hours, whereas GBCA and iodinated CT agents become distributed in the extracellular fluid space (15 L in a typical adult) within minutes (24). Because ferumoxytol has a T1 relaxivity ($\sim$15 $mmol^{-1} \cdot sec^{-1}$ at 1.5 T) that is several times that of current macrocyclic GBCAs ($\sim$3.5–5.5 $mmol^{-1} \cdot sec^{-1}$ at 1.5 T) and remains within the blood pool ($\sim$5 L in a typical adult), its potency in enhancing blood vessels persists even when it has become distributed throughout the intravascular space. This distinct feature of ferumoxytol eliminates the need to time a contrast agent bolus for a variety of vascular imaging applications and makes it practical to repeat breath-hold imaging if the first (or subsequent) attempt is unsuccessful. The uniform and complete distribution of ferumoxytol throughout the arterial and venous beds supports comprehensive vascular imaging of the chest, abdomen, and pelvis, where arteries and veins are readily distinguished from one another on the basis of anatomy. Moreover, because ferumoxytol does not leak into the interstitial fluid space, the border between blood vessel walls and their surroundings remains sharply defined, facilitating region-growing algorithms for image postprocessing such as volume rendering. We show several examples illustrating this property below. However, within the distal lower extremities and brain, equivalent enhancement of arteries and veins poses a challenge in steady-state imaging if the vessels of interest are the arteries.

The mechanism by which ferumoxytol is metabolized extends vascular imaging access to certain patient populations. Specifically, this contrast agent is safe for patients with renal impairment of any severity (25). It also obviates current potential concerns associated with long-term deposition of GBCA for patients with chronic kidney disease or younger patients in whom repeat examinations are needed (1–3). Also, the clearance of ferumoxytol through macrophages may be helpful in identification of pathologic inflammation and nodal metastases (21,22).

Safety of Ferumoxytol Use for MRI

During its therapeutic use, ferumoxytol has been associated with reports of rare and potentially fatal hypersensitivity reactions when injected rapidly and in high dose, prompting the FDA to issue a black box warning in March 2015, at which time the label for fast injection was withdrawn (9). Since that time, ferumoxytol has been infused slowly both for therapy and off-label diagnosis, and the follow-up safety data have been reassuring. Safety data for diagnostic use have been limited to small, single-center reports until 2019 when the first results of the FeraSafe registry were published (26). The registry report included more than 3000 patients and 4000 injections, where no serious adverse events were found, and minor reactions occurred in less than 2% of injections. Self-limiting iron infusion reactions, or so-called Fishbane reactions, may occur in less than 1% of patients and manifest as skin flushing, chest pressure, back pain, abdominal pain, dyspnea, or nausea (20). It is important to recognize these symptoms as distinct from allergic reactions. With Fishbane reactions, vital signs remain stable, and treatment is supportive and reassuring. Symptoms typically resolve within minutes after the infusion is stopped and generally do not recur on resumption of slower infusion. Technologists, nurses, imaging physicians, and patients should be made aware of the typical clinical manifestations of Fishbane reactions to allow their proper identification and to avoid inappropriate and potentially harmful escalation of care. Patients who are made aware of what to expect may calmly report their symptoms to the attending physician, nurse, or technologist, and infusion will be stopped until symptoms abate. In most cases, the infusion can be resumed slowly with the patient's consent following patient evaluation and confirmation of stable vital signs, without recurrence of symptoms. Education and training are therefore crucial for the safe use of ferumoxytol, as for any intravenous contrast agent. In our local experience of more than 1500 diagnostic infusions, we have observed no serious allergic reactions to ferumoxytol and have observed typical Fishbane reactions in six patients ($\sim$0.4%) that began within 2 minutes of starting the infusion. In all patients, the infusion was stopped as soon as symptoms were reported, and vital signs

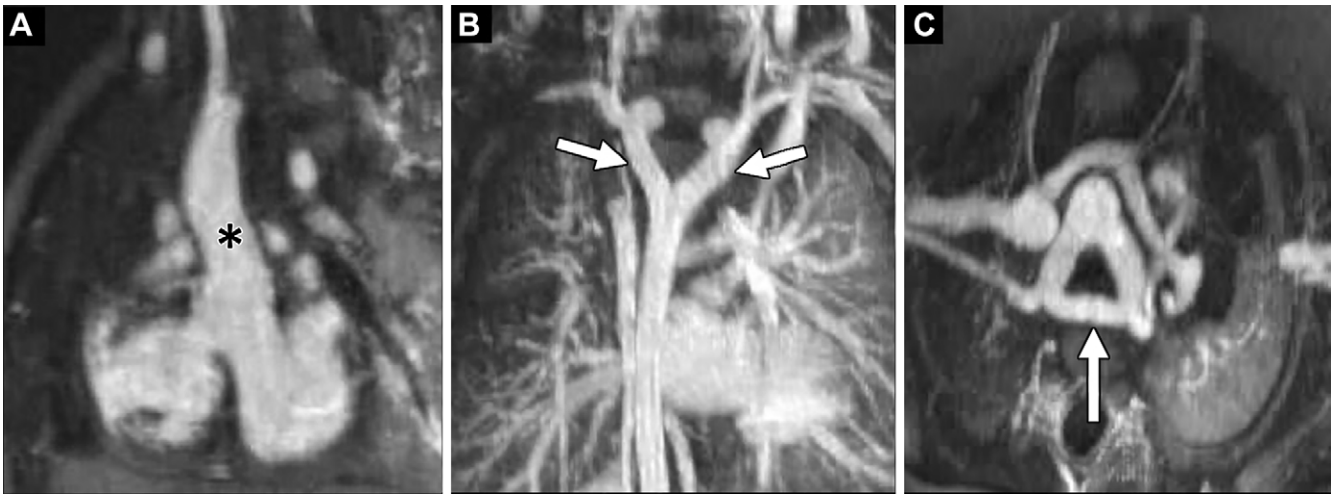

Figure 1: Ferumoxytol-enhanced MR angiography images in a 3-month-old female patient with tetralogy of Fallot and additional aortic anomalies. **(A)** Sagittal view depicts the overriding aorta (*) which is seated superior to the right and left ventricles. **(B)** Coronal view demonstrates a double aortic arch (arrows) resulting in a vascular ring around the trachea, observed on **(C)** axial view (arrow).

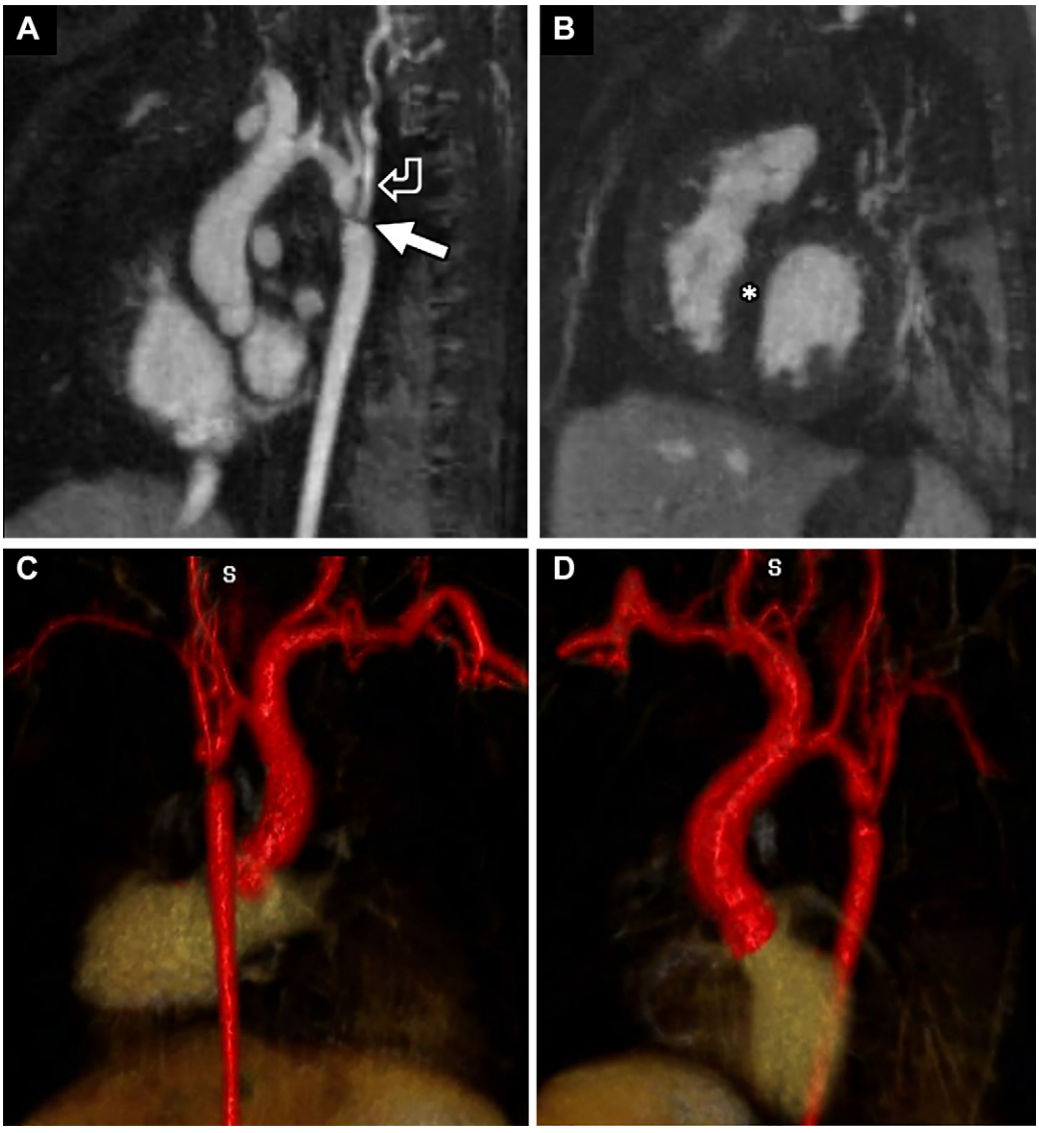

Figure 2: Ferumoxytol-enhanced MR angiography images in a 6-week-old infant with severe aortic coarctation. **(A)** Sagittal maximal intensity projection reveals the preductal aortic coarctation (arrow) near the origin of the left subclavian artery (open arrow). **(B)** The high aortic gradient resulted in left ventricular hypertrophy (*). **(C, D)** Three-dimensional volume-rendered images are useful for mapping and surgical planning. S = superior.

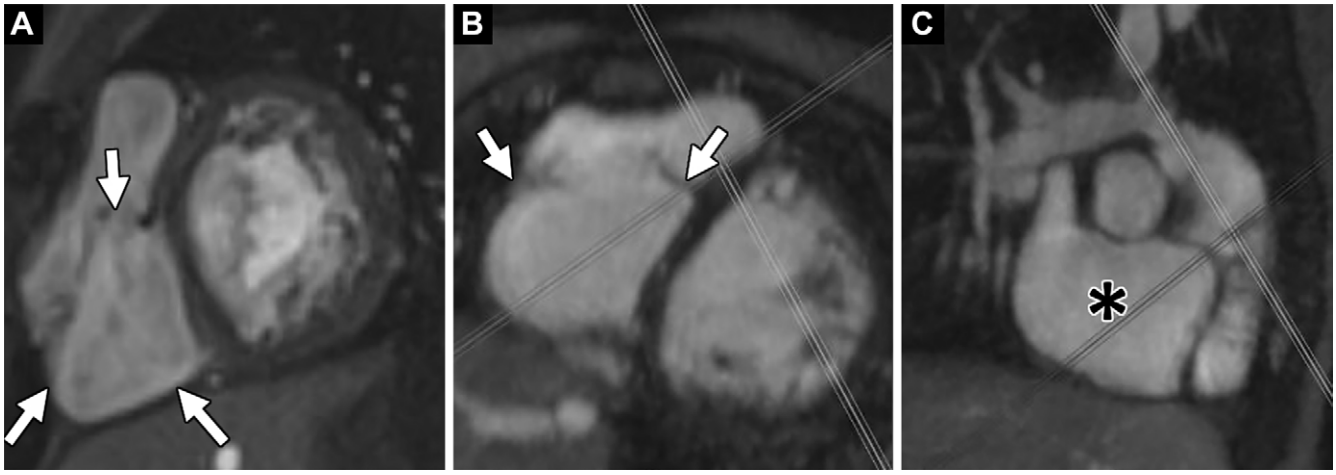

Figure 3: Ferumoxytol-enhanced MR angiography images in a young patient with Ebstein anomaly, with **(A)** a large tricuspid valve annulus (arrows), **(B)** apical displacement of the tricuspid valve leaflets (arrows), and **(C)** atrialization of a large portion of the right ventricle (*).

were stable (heart rate normal, no drop in blood pressure, no wheezing or stridor, and no drop in oxygen saturation). Symptoms included "chest tightness" or "pressure in the chest and/or abdomen," "difficulty taking a breath," flushing and redness of the skin, and "feeling bad." In all patients, symptoms resolved over 2–5 minutes once the infusion was stopped. In one patient, sufficient ferumoxytol had been delivered to complete a diagnostic examination. In three patients, the infusion was resumed slowly without recurrence of symptoms, enabling a fully diagnostic study. In two patients, the patient or parent was unwilling to resume the infusion after symptoms resolved, and the study was not diagnostic. We note that of the 1500 ferumoxytol studies performed in our institution, approximately 140 were in children under anesthesia. No adverse reactions were noted in any of these patients, but clearly, they would not have experienced (or complained of) symptoms that were not accompanied by changes in vital signs. We also note, anecdotally, that our patients who experienced Fishbane reactions were younger (typically 35 years old or younger) and in generally good health. The tolerance of ferumoxytol infusion among our older patients was excellent.

Vascular Imaging Applications

In the post–nephrogenic systemic fibrosis era, use of ferumoxytol as a contrast agent was first reported for evaluation of arteriovenous fistula patency in patients with chronic renal failure (10,20). Others explored its use for vascular imaging and transplant rejection evaluation (26,27). Patients with vascular diseases frequently have some degree of renal insufficiency, raising the bar for the use of GBCA or iodinated contrast agents. In these situations, ferumoxytol is a promising option with wide-ranging applications.

Congenital Heart Disease

CHDs, whether diagnosed early in childhood or discovered later in life, may require extensive and detailed imaging for diagnosis and treatment planning. CHD is often associated with multiple anomalies; hence, comprehensive assessment of the cardiovascular system is necessary (28). Ferumoxytol-enhanced imaging in CHD supports anatomic and functional assessment of the heart and related vascular structures. Because CHD is usually first diagnosed in childhood, conventional MRI with GBCA is challenging because of the need for a timed bolus in sync with breath holding. With traditional MRI in pediatric CHD, the presence of a highly skilled technologist and a supervising physician is a requirement during the procedure that likely will exceed an hour with repeated breath holding. Moreover, artifacts or noncompliance may require repeat imaging. In some institutions, ferumoxytol has greatly reduced the complexity and duration of image acquisition in pediatric CHD (29). If needed, imaging can be performed hours after contrast material administration, when the patient is calm, fed, or even asleep (30,31).

Multiphase steady-state imaging with contrast enhancement (MUSIC) is a four-dimensional technique used successfully with ferumoxytol in several centers for high-resolution MRI of the heart in anesthetized children (Figs 1–4). MUSIC takes advantage of the regular breathing pattern in ventilated patients to combine effective respiratory gating with cardiac gating (32). Four-dimensional MUSIC images have shown more precision and accuracy than both first-pass ferumoxytol images and conventional two-dimensional cines (32,33). With the four-dimensional approach, examination time can be shortened to about 30 minutes compared with conventional breath-hold cine and MRA, which may take 60–90 minutes. The use of ferumoxytol also improves the contrast-to-noise ratio for four-dimensional flow measurements (34–36). MRA with ferumoxytol is compatible with both 1.5-T and 3.0-T MRI systems. Despite the advantages of higher signal-to-noise ratio and lower fat signal at 3.0 T, high-quality studies can be performed routinely at both field strengths (31).

Beyond the direct consequences of abnormal cardiac structure, congenital conditions such as tetralogy of Fallot (Fig 1), aortic coarctation (Fig 2), Ebstein anomaly (Fig 3), and total anomalous pulmonary venous return (TAPVR) (Fig 4) may have indirect effects on downstream structures or organs that require evaluation. For example, with aortic coarctation, evaluation of the collaterals supplying the poststenotic segment is important.

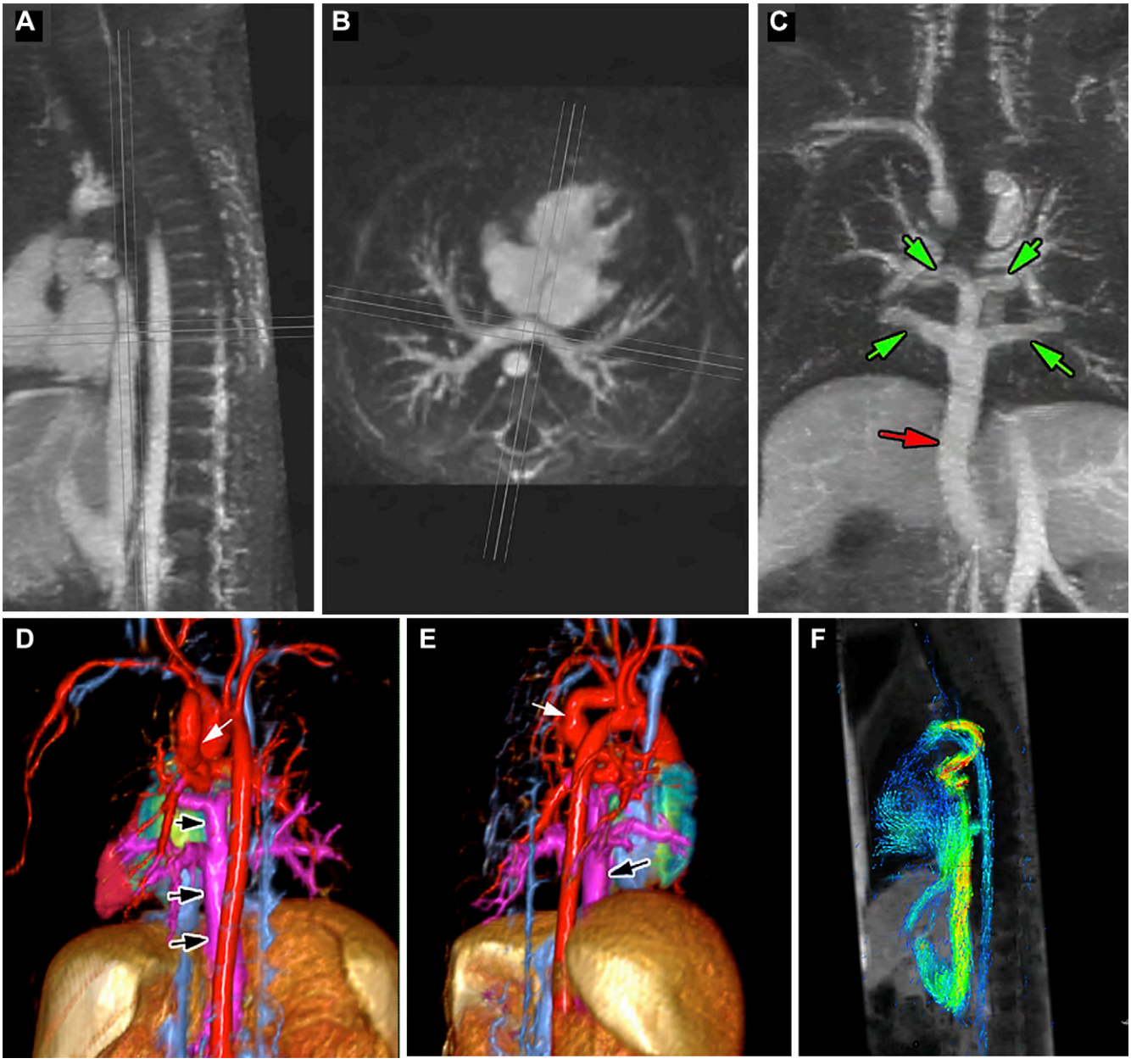

Figure 4: In total anomalous pulmonary venous return (TAPVR), all pulmonary veins drain to the systemic or portal circulation. **(A–C)** Ferumoxytol-enhanced MR angiography images in a 2-day-old, 1.9-kg male infant with infradiaphragmatic TAPVR show the pulmonary veins (green arrows) draining to the portal vein (red arrow). **(D, E)** Three-dimensional volume-rendered reconstructed images in this patient show a vertical vein rendered in red (black arrows) draining from the pulmonary venous confluence to the portal vein rendered in magenta. Additionally, this patient has pulmonary atresia with a patent ductus arteriosus supplying the pulmonary artery (white arrows). **(F)** Sagittal four-dimensional flow image shows inferiorly directed flow visualized from the vertical vein to the portal vein.

Similarly, presence of a patent ductus arteriosus in TAPVR should be identified, and the portal system must be thoroughly inspected (28,37). Ferumoxytol-enhanced MRI enables confident assessment of every vascular structure relevant for primary diagnosis, management, preoperative planning, and posttreatment surveillance. Evaluation of Fontan graft patency can be particularly challenging with GBCAs and iodinated CT agents but is straightforward with ferumoxytol MRA (Fig 5) (24,32).

Aortic Diseases

Ferumoxytol-enhanced MRA is powerful for evaluation of patients with aortic diseases, a population that tends to have coexisting renal disease (38). Many conditions are associated with slow or variable contrast bolus enhancement patterns at CT or conventional MRA (eg, aneurysms in elderly patients, dissections with differential enhancement rates for true and false lumens, and aortic stent grafts with endoleaks). In such cases, steady-state imaging with ferumoxytol guarantees that all lumens that can be enhanced are enhanced, as illustrated in several cases below.

Because the border between the vessel wall and its surroundings is typically sharp on ferumoxytol-enhanced images, region-growing algorithms perform well for three-dimensional postprocessing, such as volume rendering. Three-dimensional volume-rendered

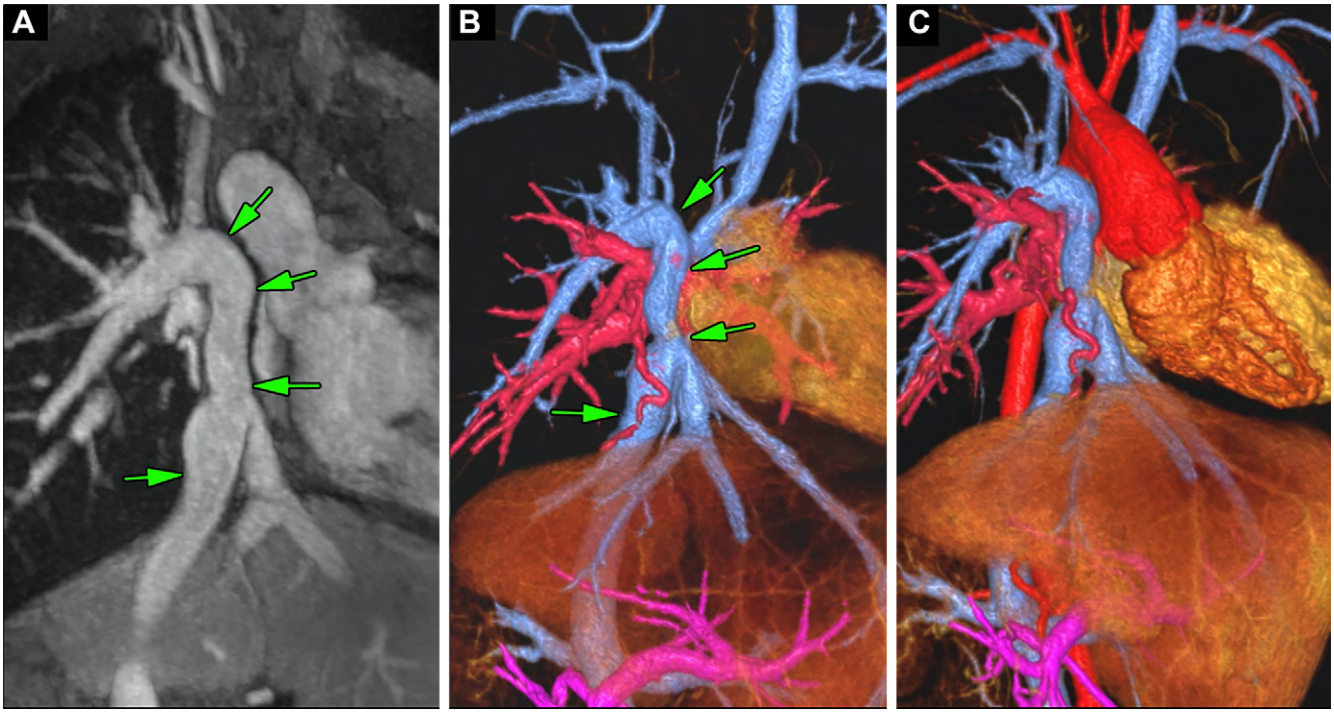

Figure 5: Ferumoxytol-enhanced MR angiography images for evaluation of a Fontan shunt in a 23-year-old patient with heterotaxia and total cavopulmonary shunt. **(A)** Coronal T1-weighted image and **(B, C)** three-dimensional volume-rendered reconstructions demonstrate a patent Fontan baffle (green arrows) that is connecting the right pulmonary artery and the inferior vena cava. **B** was rendered without the aorta and its branches for better visualization of the Fontan (compare with **C**).

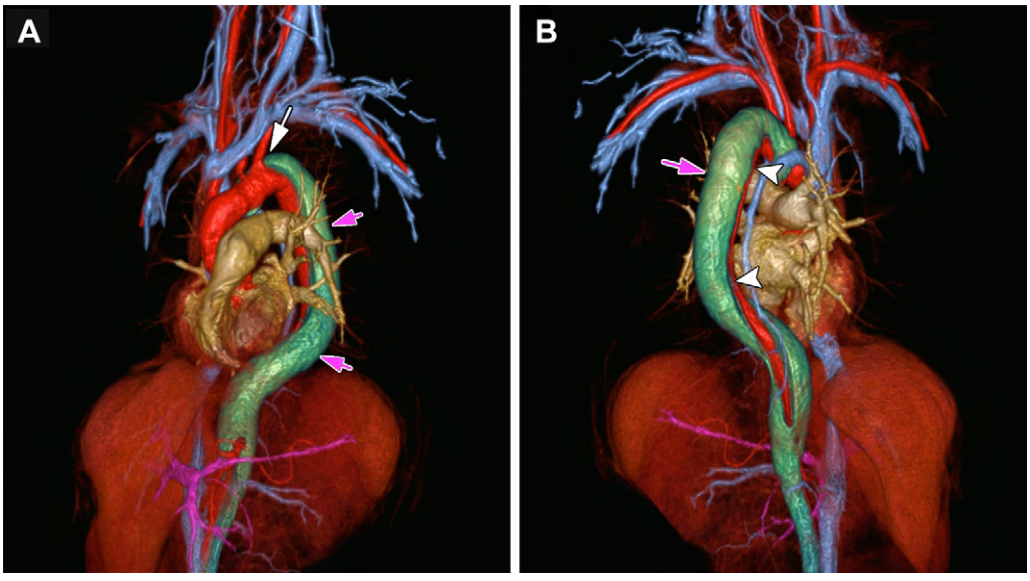

Figure 6: Three-dimensional volume-rendered reconstructions of ferumoxytol-enhanced MR angiography images with **(A)** anterior and **(B)** posterior projections of the thoracic aorta. These images demonstrate type B aortic dissection with arch involvement. The entry tear of the dissection is just distal to the origin of the left subclavian artery (white arrow, **A**). Postprocessing color rendering clearly demarcates the true lumen in red (white arrowheads) and false lumen in green (magenta arrows).

reconstructions are helpful visual tools for assessing the origin and the extent of aortic dissections (Fig 6). If stents or grafts are present, evaluation for graft patency and endoleaks is also feasible (39) (Figs 7, 8). Moreover, incorporation of iron nanoparticles into plaques has been noted in vessel wall inflammation (40).

Similar protocols and postprocessing techniques can be used when evaluating aortic aneurysms with ferumoxytol. Imaging in the steady state eliminates the requirement for bolus timing and simplifies the examination, which may be completed in as little as 5 minutes if required (41,42) (Fig 9). In the past, it has been reported that intraluminal thrombus can be visualized because of leukocyte phagocytosis of iron particles at the luminal interface of thrombus (43).

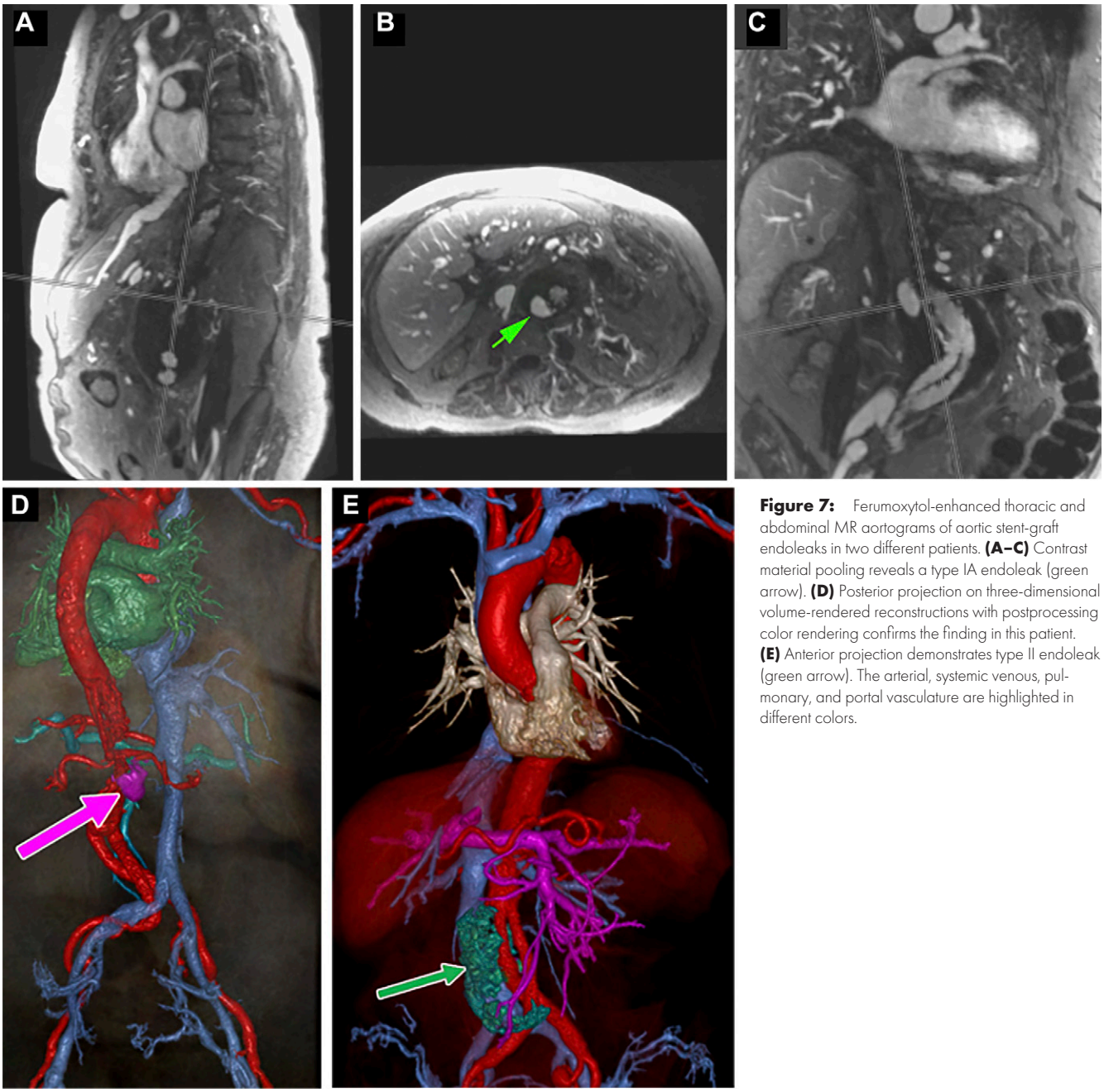

Figure 7: Ferumoxytol-enhanced thoracic and abdominal MR aortograms of aortic stent-graft endoleaks in two different patients. **(A–C)** Contrast material pooling reveals a type IA endoleak (green arrow). **(D)** Posterior projection on three-dimensional volume-rendered reconstructions with postprocessing color rendering confirms the finding in this patient. **(E)** Anterior projection demonstrates type II endoleak (green arrow). The arterial, systemic venous, pulmonary, and portal vasculature are highlighted in different colors.

Ferumoxytol-enhanced MRA has been used successfully for preprocedural workup in candidates for transcatheter aortic valve replacement. Nguyen et al (44) and Yoshida et al (45) demonstrated that the uniform intravascular enhancement provides reliable vessel diameter measurements, comprehensive vascular access-site evaluation, and vascular calcified plaque burden assessment when paired with complementary overlaid nonenhanced CT images.

Pulmonary Vasculature

In CTA evaluation of pulmonary arteries, contrast bolus timing is essential for optimal enhancement of the pulmonary arterial tree and terminal branches. In addition, respiratory motion artifacts from patients with dyspnea may limit the study. Ferumoxytol-enhanced MRA provides uniform enhancement of the pulmonary arterial system and allows for repeat imaging without bolus timing or ionizing radiation (Fig 10) (46). Bedayat et al reported superior opacification of pulmonary arteries compared with arterial phase GBCA-enhanced MRA, and of the pulmonary arteries, pulmonary veins, inferior vena cava, and superior vena cava compared with venous phase GBCA-enhanced MRA (47). An earlier study using a different ultrasmall superparamagnetic iron oxide agent reported that respiratory gating can be successfully applied for acquisition of pulmonary vascular images (48). A recent study by Khan et al found that ferumoxytol-enhanced MRA may outperform CTA for evaluation of treated arteriovenous malformations (49).

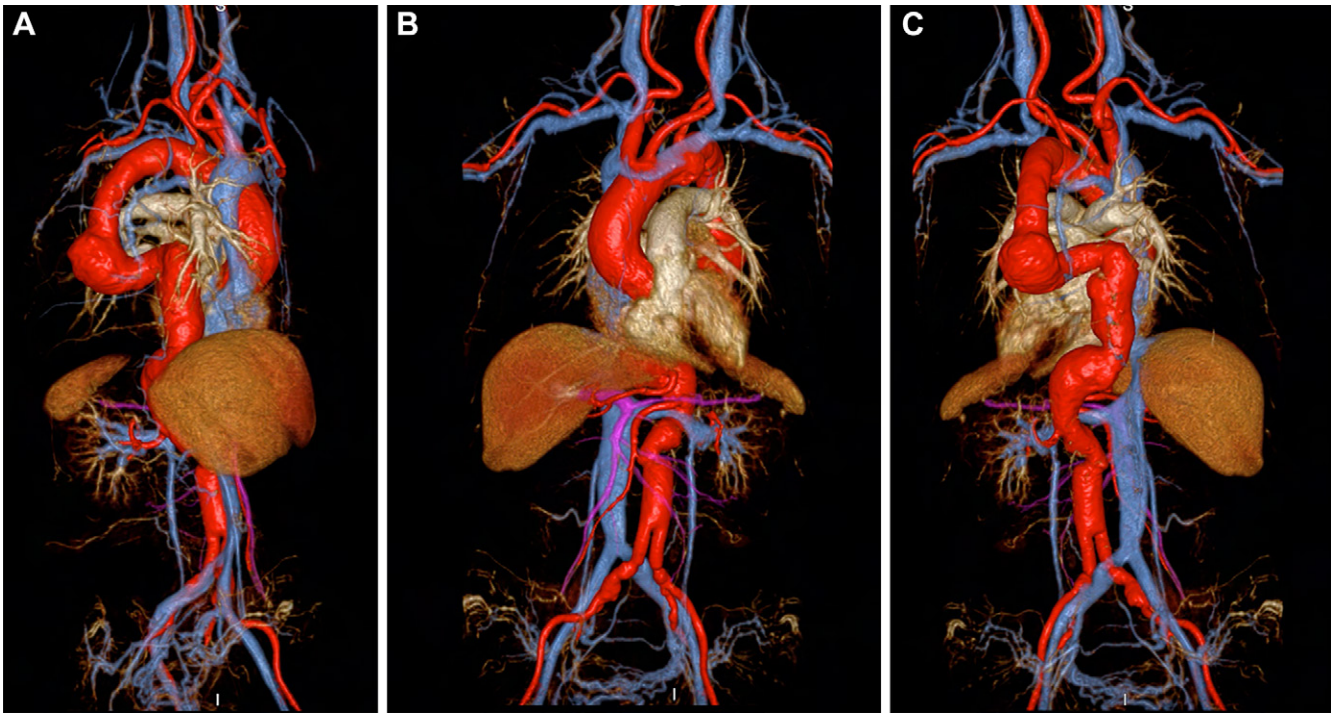

Figure 8: Three-dimensional volume-rendered reconstructed ferumoxytol-enhanced MR angiography images of the chest, abdominal, and pelvic vascular systems, with systemic arteries in red, veins in blue, pulmonary vascular tree in tan, and portal system in magenta. The image has been rotated for **(A)** right sagittal, **(B)** anterior, and **(C)** posterior oblique views. Multiple aneurysms of the tortuous thoracoabdominal aorta, as well as a patent aortoiliac surgical graft, can be observed.

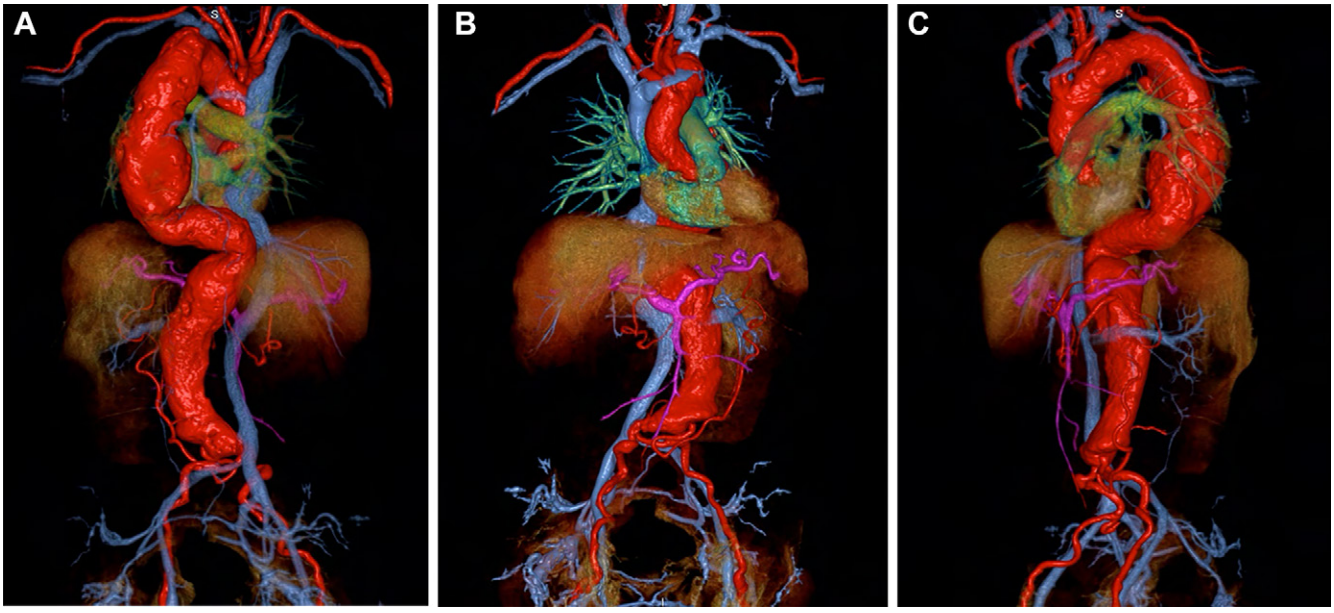

Figure 9: Three-dimensional volume-rendered reconstructed ferumoxytol-enhanced MR angiography images of the chest, abdominal, and pelvic vascular systems, with systemic arteries in red, veins in blue, pulmonary vascular tree in green, and portal system in magenta. The image has been rotated for **(A)** posterior, **(B)** anterior, and **(C)** left posterior oblique views. Systemic veins, pulmonary veins, and portal system have been dampened in **A** and **C** to increase conspicuity of the systemic arterial vasculature, which shows a large thoracoabdominal aortic aneurysm.

Patients with Renal Insufficiency

Patients with renal insufficiency frequently require repeated contrast-enhanced imaging for a variety of indications, including vascular mapping for arteriovenous fistulae or grafts and preoperative planning or evaluation of transplant renal arteries (10,50).

US assessment may be limited if detailed procedural planning is required (51). Unenhanced time-of-flight MRA is sometimes performed but is vulnerable to artifacts from blood flow in tortuous and complex vascular anatomy. Limitations from nephrotoxicity of conventional contrast agents for CTA and concern for systemic fibrosis from

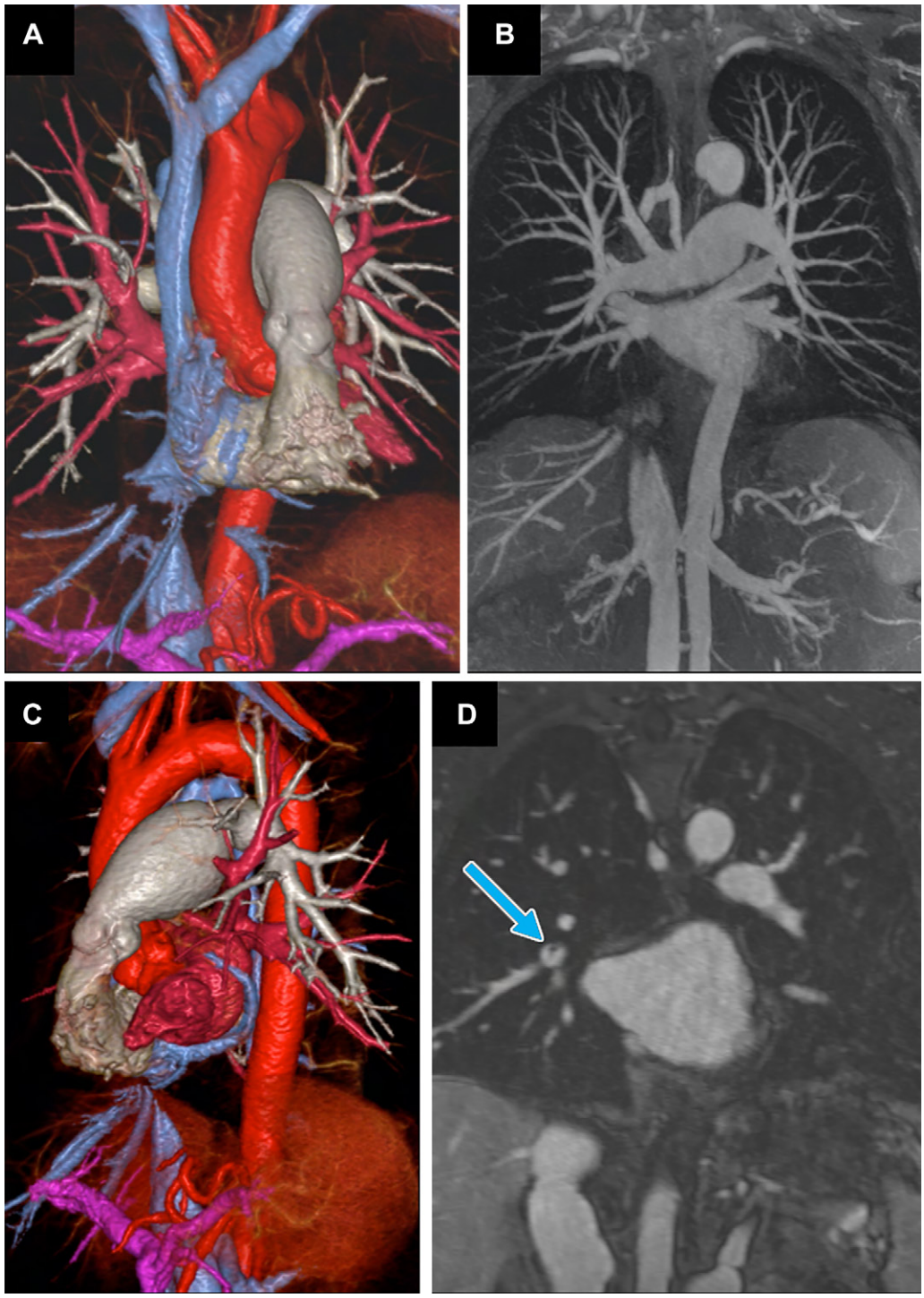

Figure 10: Ferumoxytol-enhanced MR angiography coronal T1-weighted and three-dimensional reconstruction images demonstrate simultaneous enhancement of pulmonary and systemic arteries and veins **(A–C)** in a patient with normal vasculature and **(D)** in a patient with an acute right interlobar pulmonary arterial embolus (blue arrow).

GBCA-enhanced MRI pose challenges for evaluation of patients with renal insufficiency (10). Group II GBCAs carry less theoretical nephrogenic systemic fibrosis risk (0.07%), but larger studies are needed to confirm this finding (52,53).

Ferumoxytol offers an alternative pathway for these patients to undergo vascular imaging, without nephrotoxicity concerns (Figs 11, 12) (10,54,55).

Vascular Occlusions and Stress Imaging

It is now well established that ferumoxytol can evaluate the extent and location of vascular thrombus or stenosis, as well as collateral vessel development, even in situations where the washout dynamics of GBCA may be problematic (Figs 13, 14) (56). Additionally, in deep venous thrombosis, venography and pulmonary embolism assessment can be performed simultane-

ously (57). Studies have found additional thrombosed sites when compared with Doppler US results (58). With steady-state ferumoxytol-enhanced imaging of the extremity vessels, simultaneous enhancement of arteries, veins, and collaterals can be challenging but is the focus of ongoing work (Fig 13).

Ferumoxytol-enhanced studies can be distinctly useful for provocative stress maneuvers. Because of the stable intravascular signal, any imaging changes between maneuvers can be ascribed solely to the maneuver. For example, Figure 15 demonstrates popliteal vessel compression during plantar flexion, suggestive of popliteal entrapment syndrome. As another example, Figure 16 demonstrates narrowing of the celiac artery at the proximal ostium from end inspiration to end expiration, suggestive of median arcuate ligament compression. Traditionally, contrast-enhanced dynamic imaging with GBCA requires two separately timed injections and acquisitions, one in the relaxed position and another with the desired maneuver or posture. With ferumoxytol, multiple acquisitions can be obtained in a steady state following a single injection, with no changes in the images other than those due to the stress maneuver. A wide array of possible provocative imaging applications may become feasible using this approach. A recent study investigated the use of ferumoxytol-enhanced abdominal MRA with meal challenges to diagnose and locate chronic mesenteric ischemia in patients with ambiguous abdominal pain after meals (59).

Conclusion

A growing body of evidence suggests that ferumoxytol is a safe and effective contrast agent for many vascular MRI applications. It is clearly an option for patients in whom iodinated agents or GBCAs may be contraindicated. The pharmacokinetics and relaxivity of ferumoxytol make it distinctly powerful for vascular imaging, providing high-quality anatomic and functional information while simplifying image acquisition and workflow. Vascular applications include evaluation of complex arterial and venous anatomy, CHD, and imaging of inducible vascular compression.

Obstacles to the more widespread use of ferumoxytol have included its high cost, availability limited to the United States, and the lack of a diagnostic label. However, the approval of a generic version of ferumoxytol (Covis Pharma) in July 2021 has already resulted in substantial price reduction. Moreover, as costs diminish and more data on the safe and effective use of ferumoxytol become available, the hope is that this versatile agent will become widely available for use in appropriate patient groups.

Author contributions: Guarantors of integrity of entire study, **J.P.F., A.B.**; study concepts/study design or data acquisition or data analysis/interpretation, all authors; manuscript drafting or manuscript revision for important intellectual content, all

Figure 11: High-resolution three-dimensional volume-rendered ferumoxytol-enhanced MR angiography image demonstrates a left upper extremity hemodialysis fistula with a dilated, aneurysmal venous limb (open arrows). Proximally, there are collateral vessels (arrow). More proximally, there is stenosis of the left subclavian vein just distal to the internal jugular vein junction (arrowhead). The left brachiocephalic vein is relatively collapsed. This constellation of findings represents venous obstruction at the site of left subclavian vein stenosis. S = superior.

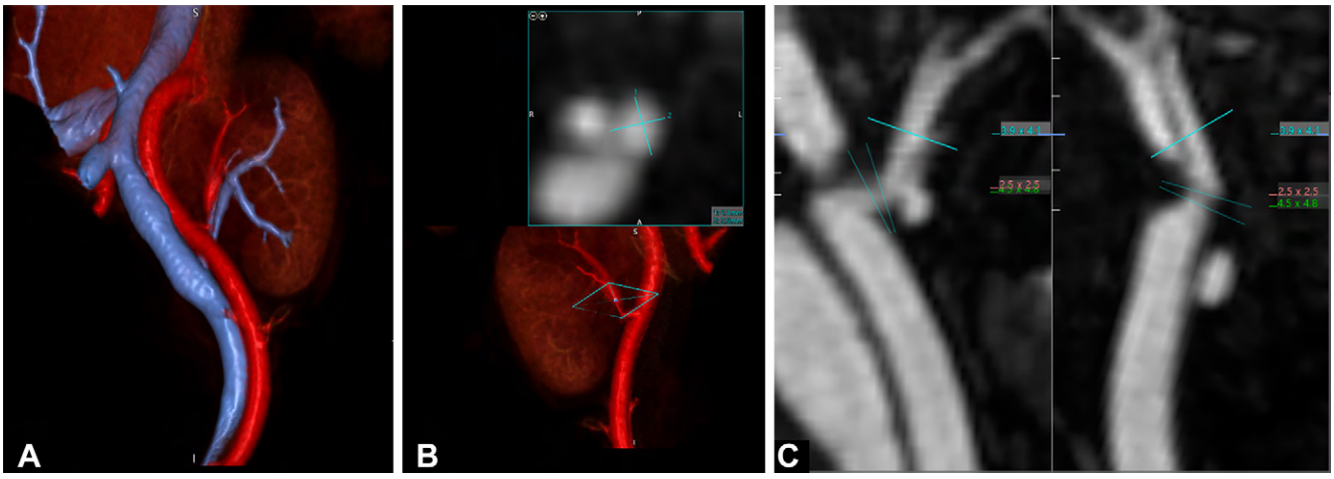

Figure 12: Ferumoxytol-enhanced MR angiography images in a patient with a left lower quadrant renal transplant. **(A, B)** Three-dimensional volume-rendered reconstructions and **(C)** coronal blood pool image demonstrate focal narrowing of the renal artery to 3–4 mm just proximal to the anastomosis site.

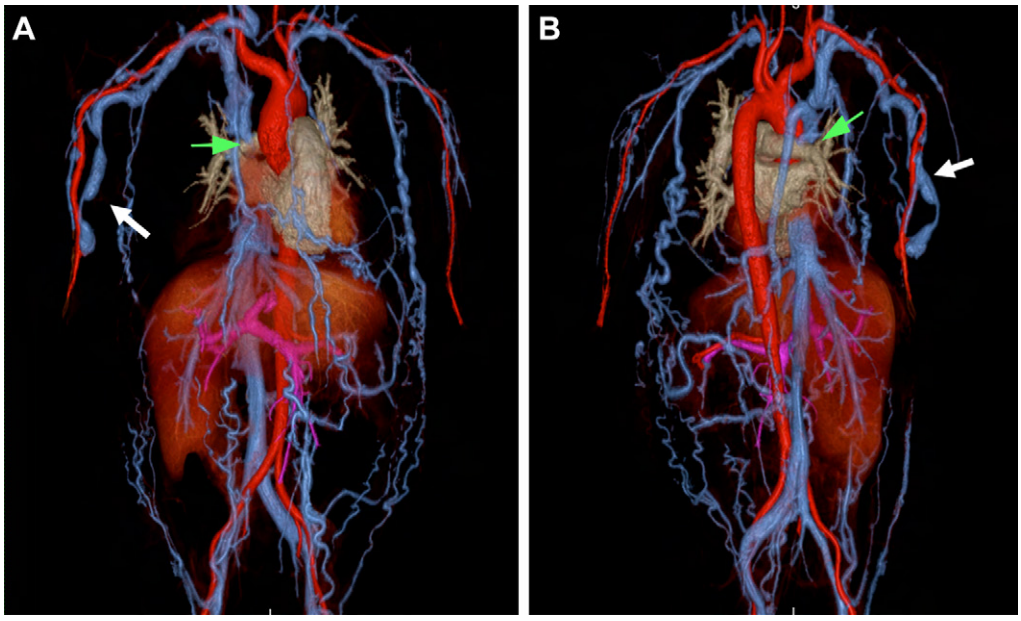

Figure 13: Three-dimensional volume-rendered ferumoxytol-enhanced MR angiography of the chest, abdomen, and pelvis with **(A)** anterior and **(B)** posterior projections obtained in two overlapping breath-hold acquisitions. The images demonstrate an occluded superior vena cava (green arrows) and development of collateral vessels. In **B**, the inferior vena cava and hepatic veins are clearly patent. The pulmonary vessels (tan color) and portal vasculature (magenta) were made more transparent during post-processing to emphasize the systemic arterial (red) and venous (blue) vasculature. Incidentally, the patient's hemodialysis fistula is visualized in the right upper extremity (white arrows).

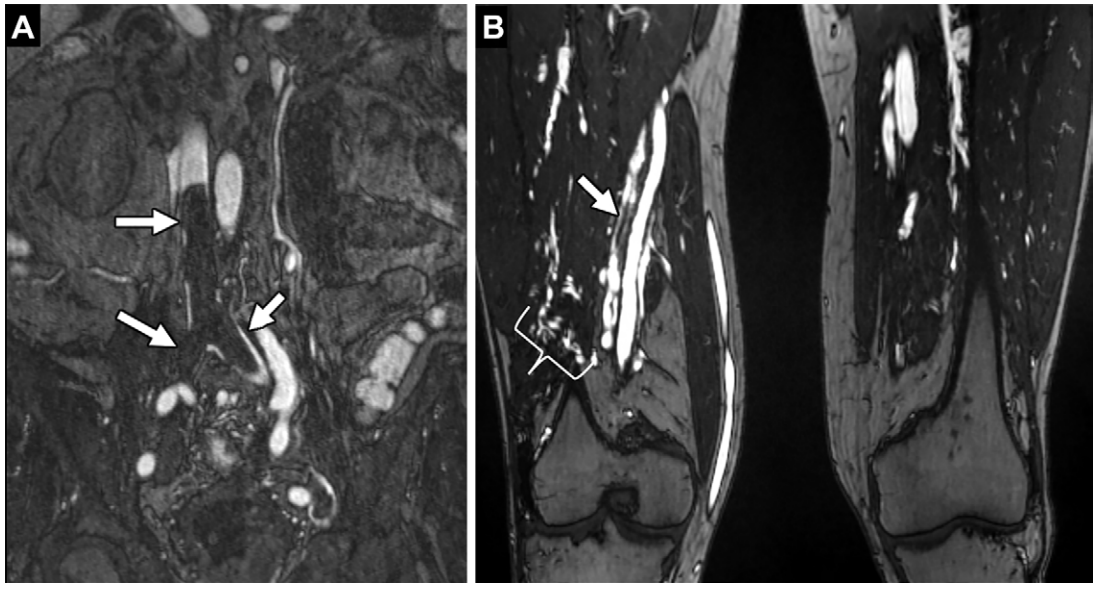

Figure 14: Coronal ferumoxytol-enhanced T1-weighted MR angiography (MRA) images in two different patients with deep venous thrombosis (DVT). **(A)** MR angiogram of the abdomen-pelvis shows a central filling defect extending from the inferior vena cava to the common iliac veins (arrows) with no significant collaterals, compatible with acute DVT. **(B)** MR angiogram of the lower extremities shows a central linear filling defect within the right mid distal femoral vein (arrow) with associated collateral vessel formation (bracket), suggestive of chronic DVT. Note the uniform opacification of the collateral vessels with ferumoxytol, which would be difficult to visualize using gadolinium-based contrast agents due to contrast washout dynamics.

authors; approval of final version of submitted manuscript, all authors; agrees to ensure any questions related to the work are appropriately resolved, all authors; literature research, all authors; clinical studies, **M.H.J., J.P.F.**; and manuscript editing, all authors

Disclosures of conflicts of interest: M.H.J. No relevant relationships. **T.Y.** No relevant relationships. **C.H.** No relevant relationships. **A.E.P.** All grant funding is entirely unrelated to this manuscript: September 20, 2016 to August 31, 2021 calendar: Boston University/NIH –NCI prime (R01CA210360), $1 646 404 total, Molecular and Imaging Biomarkers for Early Lung Cancer Detection in the Setting of Indeterminate Pulmonary Nodules, role: investigator; September 1, 2020 to August 31, 2021 calendar: American College of Radiology $100 000 total, Lung Cancer Screening in African Americans, A Community Engagement Project, role: principal investigator; January 1, 2020 to March 31, 2022 calendar: American Col-

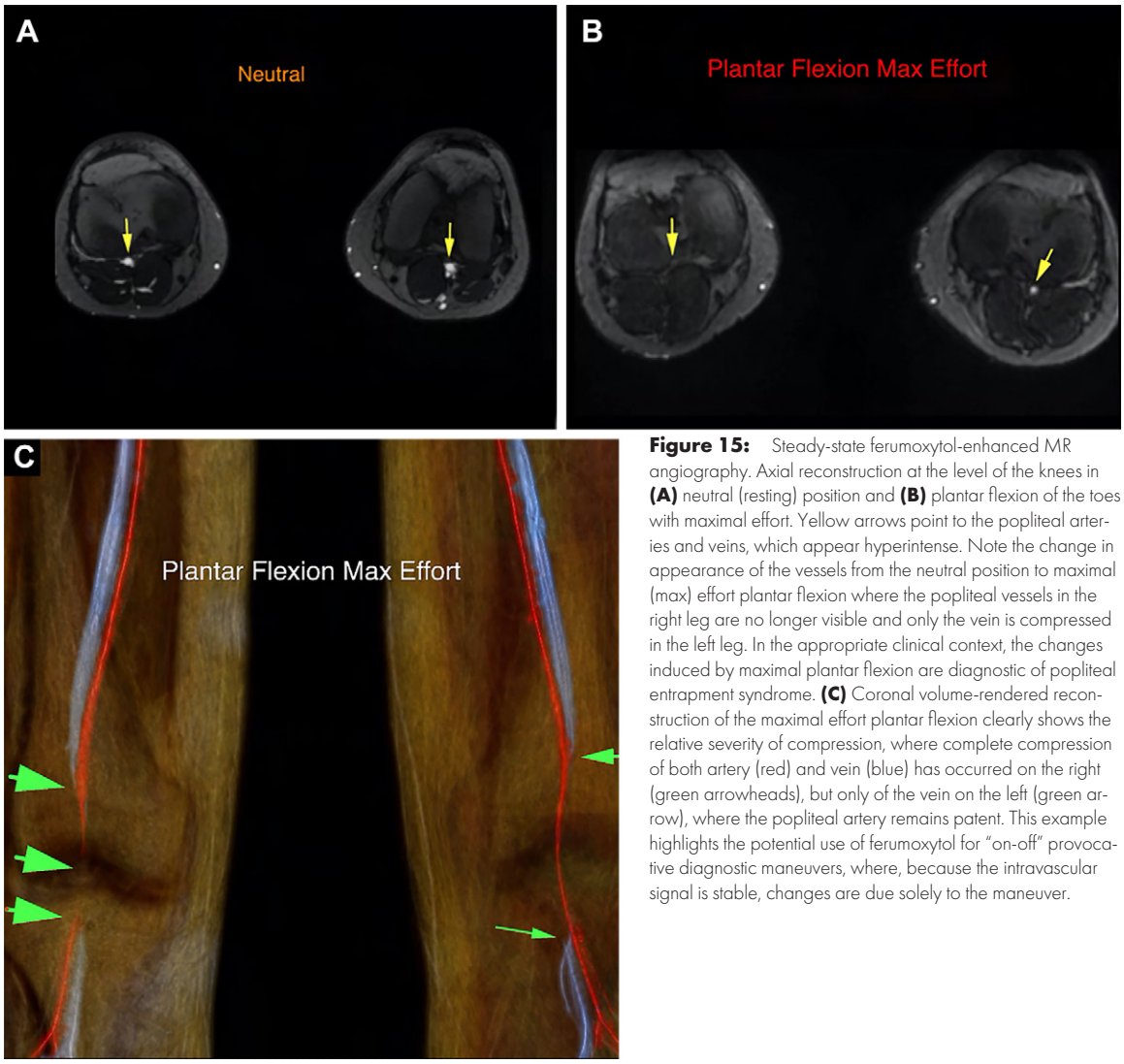

Figure 15: Steady-state ferumoxytol-enhanced MR angiography. Axial reconstruction at the level of the knees in **(A)** neutral (resting) position and **(B)** plantar flexion of the toes with maximal effort. Yellow arrows point to the popliteal arteries and veins, which appear hyperintense. Note the change in appearance of the vessels from the neutral position to maximal (max) effort plantar flexion where the popliteal vessels in the right leg are no longer visible and only the vein is compressed in the left leg. In the appropriate clinical context, the changes induced by maximal plantar flexion are diagnostic of popliteal entrapment syndrome. **(C)** Coronal volume-rendered reconstruction of the maximal effort plantar flexion clearly shows the relative severity of compression, where complete compression of both artery (red) and vein (blue) has occurred on the right (green arrowheads), but only of the vein on the left (green arrow), where the popliteal artery remains patent. This example highlights the potential use of ferumoxytol for "on-off" provocative diagnostic maneuvers, where, because the intravascular signal is stable, changes are due solely to the maneuver.

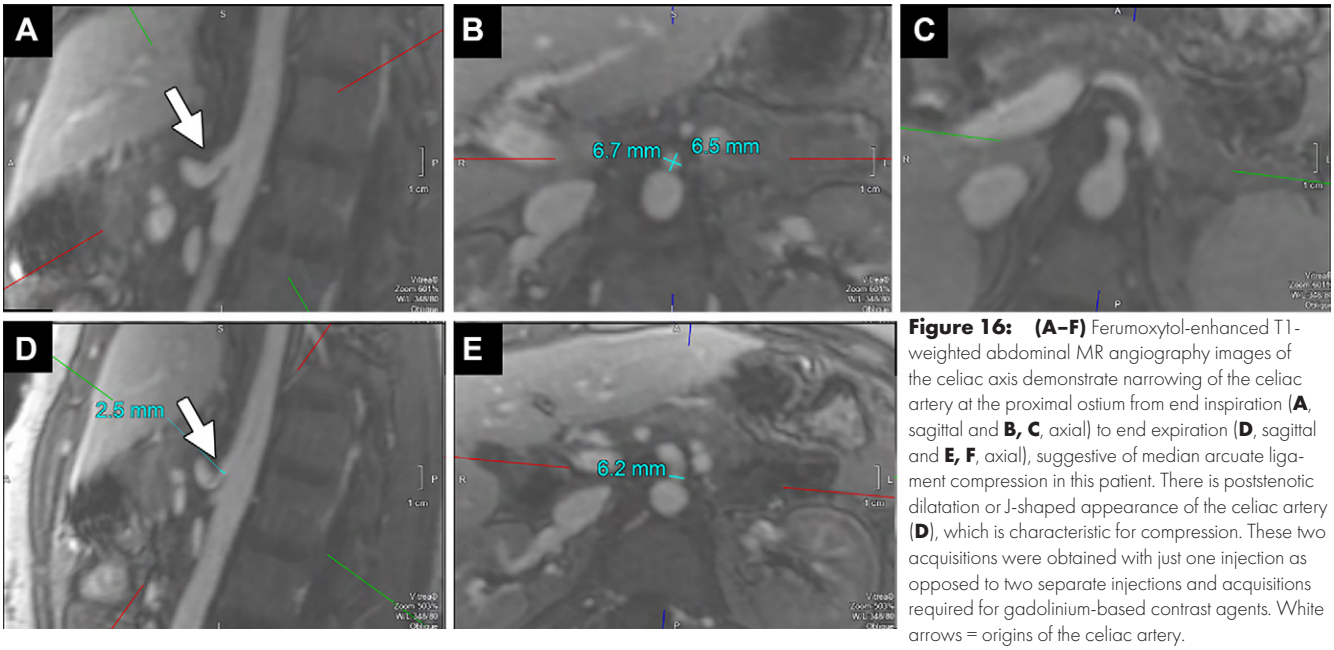

Figure 16: **(A–F)** Ferumoxytol-enhanced T1-weighted abdominal MR angiography images of the celiac axis demonstrate narrowing of the celiac artery at the proximal ostium from end inspiration (**A**, sagittal and **B, C**, axial) to end expiration (**D**, sagittal and **E, F**, axial), suggestive of median arcuate ligament compression in this patient. There is poststenotic dilatation or J-shaped appearance of the celiac artery (**D**), which is characteristic for compression. These two acquisitions were obtained with just one injection as opposed to two separate injections and acquisitions required for gadolinium-based contrast agents. White arrows = origins of the celiac artery.

lege of Radiology $196 275, DECAMP-1 PLUS: Predication of Lung cancer using Noninvasive Biomarkers, role: site principal investigator; June 17, 2019 to July 8, 2023 calendar: Edwards Lifesciences $11 673 total (to date), Multicenter Trial of Congenital Pulmonic Valve Dysfunction Studying the SAPIEN 3 Interventional THV with the Alterra Adaptive Prestent. This is a clinical trial evaluating the SAPIEN 3 transcatheter valve, role: investigator; April 2, 2019 to March 31, 2020 calendar: Stanford/NIH-NHLBI $237 111 total (to date) NCTE pending, Validating Cardiac MRI Biomarkers and Genotype-Phenotype Correlations for DMD, role: investigator; consulting fees from MedQIA; payment for speaking honoraria from Los Angeles Radiological Society; travel support from Siemens to give a lecture (2019); American College of Radiology Council Steering Committee. **J.P.F.** NIH 2R01 HL127153-06 (not relevant). **A.B.** No relevant relationships.

References

1. Stojanov D, Aracki-Trenkic A, Benedeto-Stojanov D. Gadolinium deposition within the dentate nucleus and globus pallidus after repeated administrations of gadolinium-based contrast agents-current status. Neuroradiology 2016;58(5):433–441.
2. McDonald RJ, McDonald JS, Kallmes DF, et al. Gadolinium deposition in human brain tissues after contrast-enhanced MR imaging in adult patients without intracranial abnormalities. Radiology 2017;285(2):546–554.
3. Kralik SF, Singhal KK, Frank MS, Ladd LM. Evaluation of Gadolinium Deposition in the Brain After MR Arthrography. AJR Am J Roentgenol 2018;211(5):1063–1067.
4. Granata V, Cascella M, Fusco R, et al. Immediate adverse reactions to gadolinium-based MR contrast media: A retrospective analysis on 10,608 examinations. BioMed Res Int 2016;2016:3918292.
5. Kuo PH, Kanal E, Abu-Alfa AK, Cowper SE. Gadolinium-based MR contrast agents and nephrogenic systemic fibrosis. Radiology 2007;242(3):647–649.
6. Kanda T, Fukusato T, Matsuda M, et al. Gadolinium-based contrast agent accumulates in the brain even in subjects without severe renal dysfunction: Evaluation of autopsy brain specimens with inductively coupled plasma mass spectroscopy. Radiology 2015;276(1):228–232.
7. Edelman RR, Koktzoglou I. Noncontrast MR angiography: An update. J Magn Reson Imaging 2019;49(2):355–373.
8. Hassan N, Boville B, Reischmann D, Ndika A, Sterken D, Kovey K. Intravenous Ferumoxytol in Pediatric Patients With Iron Deficiency Anemia. Ann Pharmacother 2017;51(7):548–554.
9. AMAG Pharmaceuticals. Feraheme [prescribing information]. https://www.accessdata.fda.gov/drugsatfda_docs/label/2018/022180s009lbl.pdf. Revised February 2018. Accessed January 28, 2021.
10. Sigovan M, Gasper W, Alley HF, Owens CD, Saloner D. USPIO-enhanced MR angiography of arteriovenous fistulas in patients with renal failure. Radiology 2012;265(2):584–590.
11. Li W, Tutton S, Vu AT, et al. First-pass contrast-enhanced magnetic resonance angiography in humans using ferumoxytol, a novel ultrasmall superparamagnetic iron oxide (USPIO)-based blood pool agent. J Magn Reson Imaging 2005;21(1):46–52.
12. Finn JP, Nguyen KL, Hu P. Ferumoxytol vs. Gadolinium agents for contrast-enhanced MRI: Thoughts on evolving indications, risks, and benefits. J Magn Reson Imaging 2017;46(3):919–923.
13. Turkbey B, Czarniecki M, Shih JH, et al. Ferumoxytol-enhanced MR lymphography for detection of metastatic lymph nodes in genitourinary malignancies: A prospective study. AJR Am J Roentgenol 2020;214(1):105–113.
14. Yilmaz A, Dengler MA, van der Kuip H, et al. Imaging of myocardial infarction using ultrasmall superparamagnetic iron oxide nanoparticles: a human study using a multi-parametric cardiovascular magnetic resonance imaging approach. Eur Heart J 2013;34(6):462–475.
15. Li W, Salanitri J, Tutton S, et al. Lower extremity deep venous thrombosis: evaluation with ferumoxytol-enhanced MR imaging and dual-contrast mechanism--preliminary experience. Radiology 2007;242(3):873–881.
16. Dósa E, Guillaume DJ, Haluska M, et al. Magnetic resonance imaging of intracranial tumors: intra-patient comparison of gadoteridol and ferumoxytol. Neuro Oncol 2011;13(2):251–260.
17. Muehe AM, Siedek F, Theruvath AJ, et al. Differentiation of benign and malignant lymph nodes in pediatric patients on ferumoxytol-enhanced PET/MRI. Theranostics 2020;10(8):3612–3621.
18. Huang Y, Singer TG, Iv M, et al. Ferumoxytol-enhanced MRI for surveillance of pediatric cerebral arteriovenous malformations. J Neurosurg Pediatr 2019;24(4):407–414.
19. Ning P, Zucker EJ, Wong P, Vasanawala SS. Hemodynamic safety and efficacy of ferumoxytol as an intravenous contrast agents in pediatric patients and young adults. Magn Reson Imaging 2016;34(2):152–158.
20. Finn JP, Nguyen KL, Han F, et al. Cardiovascular MRI with ferumoxytol. Clin Radiol 2016;71(8):796–806.
21. Corot C, Robert P, Idée JM, Port M. Recent advances in iron oxide nanocrystal technology for medical imaging. Adv Drug Deliv Rev 2006;58(14):1471–1504.
22. Kordbacheh H, Baliyan V, Parakh A, Wojtkiewicz GR, Hedgire S, Harisinghani MG. Pictorial review on abdominal applications of ferumoxytol in MR imaging. Abdom Radiol (NY) 2019;44(10):3273–3284.
23. Stoumpos S, Hennessy M, Vesey AT, et al. Ferumoxytol magnetic resonance angiography: a dose-finding study in patients with chronic kidney disease. Eur Radiol 2019;29(7):3543–3552.
24. Toth GB, Varallyay CG, Horvath A, et al. Current and potential imaging applications of ferumoxytol for magnetic resonance imaging. Kidney Int 2017;92(1):47–66.
25. Vasanawala SS, Nguyen KL, Hope MD, et al. Safety and technique of ferumoxytol administration for MRI. Magn Reson Med 2016;75(5):2107–2111.
26. Johansson L, Johnsson C, Penno E, Björnerud A, Ahlström H. Acute cardiac transplant rejection: detection and grading with MR imaging with a blood pool contrast agent--experimental study in the rat. Radiology 2002;225(1):97–103.
27. Bashir MR, Mody R, Neville A, et al. Retrospective assessment of the utility of an iron-based agent for contrast-enhanced magnetic resonance venography in patients with endstage renal diseases. J Magn Reson Imaging 2014;40(1):113–118.
28. Bedayat A, Jalili MH, Hassani C, Chalian H, Reuhm S, Moriarty J. CT evaluation of unrepaired/incidental congenital cardiovascular diseases in adults. Diagn Interv Imaging 2021;102(4):213–224.
29. Nguyen KL, Ghosh RM, Griffin LM, et al. Four-dimensional Multiphase Steady-State MRI with Ferumoxytol Enhancement: Early Multicenter Feasibility in Pediatric Congenital Heart Disease. Radiology 2021;300(1):162–173.
30. Hartmann M, Wiethoff AJ, Hentrich HR, Rohrer M. Initial imaging recommendations for Vasovist angiography. Eur Radiol 2006;16(Suppl 2):B15–B23.
31. Lai LM, Cheng JY, Alley MT, Zhang T, Lustig M, Vasanawala SS. Feasibility of ferumoxytol-enhanced neonatal and young infant cardiac MRI without general anesthesia. J Magn Reson Imaging 2017;45(5):1407–1418.
32. Nguyen KL, Han F, Zhou Z, et al. 4D MUSIC CMR: value-based imaging of neonates and infants with congenital heart disease. J Cardiovasc Magn Reson 2017;19(1):40.
33. Han F, Rapacchi S, Khan S, et al. Four-dimensional, multiphase, steady-state imaging with contrast enhancement (MUSIC) in the heart: a feasibility study in children. Magn Reson Med 2015;74(4):1042–1049.
34. Cheng JY, Hanneman K, Zhang T, et al. Comprehensive motion-compensated highly accelerated 4D flow MRI with ferumoxytol enhancement for pediatric congenital heart disease. J Magn Reson Imaging 2016;43(6):1355–1368.
35. Zhou Z, Han F, Rapacchi S, et al. Accelerated ferumoxytol-enhanced 4D multiphase, steady-state imaging with contrast enhancement (MUSIC) cardiovascular MRI: validation in pediatric congenital heart disease. NMR Biomed 2017;30(1):e3663.
36. Han F, Zhou Z, Han E, et al. Self-gated 4D multiphase, steady-state imaging with contrast enhancement (MUSIC) using rotating cartesian K-space (ROCK): Validation in children with congenital heart disease. Magn Reson Med 2017;78(2):472–483.
37. Krueger JJ, Ewert P, Yilmaz S, et al. Magnetic resonance imaging-guided balloon angioplasty of coarctation of the aorta: a pilot study. Circulation 2006;113(8):1093–1100.
38. Hagiwara S, Saima S, Negishi K, et al. High incidence of renal failure in patients with aortic aneurysms. Nephrol Dial Transplant 2007;22(5):1361–1368.
39. Ersoy H, Jacobs P, Kent CK, Prince MR. Blood pool MR angiography of aortic stent-graft endoleak. AJR Am J Roentgenol 2004;182(5):1181–1186.
40. Hedgire S, Krebill C, Wojtkiewicz GR, et al. Ultrasmall superparamagnetic iron oxide nanoparticle uptake as noninvasive marker of aortic wall inflammation on MRI: proof of concept study. Br J Radiol 2018;91(1092):20180461.
41. Weishaupt D, Rühm SG, Binkert CA, et al. Equilibrium-phase MR angiography of the aortoiliac and renal arteries using a blood pool contrast agent. AJR Am J Roentgenol 2000;175(1):189–195.
42. Truijers M, Fütterer JJ, Takahashi S, Heesakkers RA, Blankensteijn JD, Barentsz JO. In vivo imaging of the aneurysm wall with MRI and a macrophage-specific contrast agent. AJR Am J Roentgenol 2009;193(5):W437–W441.
43. Nchimi A, Defawe O, Brisbois D, et al. MR imaging of iron phagocytosis in intraluminal thrombi of abdominal aortic aneurysms in humans. Radiology 2010;254(3):973–981.
44. Nguyen KL, Moriarty JM, Plotnik AN, et al. Ferumoxytol-enhanced MR angiography for vascular access mapping before transcatheter aortic valve replacement in patients with renal impairment: A step toward patient-specific care. Radiology 2018;286(1):326–337.
45. Yoshida T, Nguyen KL, Shahrouki P, Quinones-Baldrich WJ, Lawrence PF, Finn JP. Intermodality feature fusion combining unenhanced computed tomography and ferumoxytol-enhanced magnetic resonance angiography for patient-specific vascular mapping in renal impairment. J Vasc Surg 2020;71(5):1674–1684.

46. Knobloch G, Colgan T, Schiebler ML, et al. Comparison of gadolinium-enhanced and ferumoxytol-enhanced conventional and UTE-MRA for the depiction of the pulmonary vasculature. Magn Reson Med 2019;82(5):1660–1670.
47. Bedayat A, Nguyen KL, Prosper AE, Moriarty JM, Finn JP. Ferumoxytol-Enhanced MRA for Evaluation of the Pulmonary Vascular Network. In: oral presentation at: North American Society for Cardiovascular Imaging 2019 annual meeting, Seattle, WA.
48. Ahlström KH, Johansson LO, Rodenburg JB, Ragnarsson AS, Åkeson P, Börseth A. Pulmonary MR angiography with ultrasmall superparamagnetic iron oxide particles as a blood pool agent and a navigator echo for respiratory gating: pilot study. Radiology 1999;211(3):865–869.
49. Khan SN, McWilliams JP, Bista BB, Kee S, Finn JP. Comparison of Ferumoxytol-enhanced MR Angiography and CT Angiography for the Detection of Pulmonary Arteriovenous Malformations in Hereditary Hemorrhagic Telangiectasia: Initial Results. Radiol Cardiothorac Imaging 2020;2(2):e190077.
50. Gondalia R, Vernuccio F, Marin D, Bashir MR. The role of MR imaging in the assessment of renal allograft vasculature. Abdom Radiol (NY) 2018;43(10):2589–2596.
51. Bashir MR, Jaffe TA, Brennan TV, Patel UD, Ellis MJ. Renal transplant imaging using magnetic resonance angiography with a nonnephrotoxic contrast agent. Transplantation 2013;96(1):91–96.
52. Attari H, Cao Y, Elmholdt TR, Zhao Y, Prince MR. A Systematic Review of 639 Patients with Biopsy-confirmed Nephrogenic Systemic Fibrosis. Radiology 2019;292(2):376–386.
53. Woolen SA, Shankar PR, Gagnier JJ, MacEachern MP, Singer L, Davenport MS. Risk of Nephrogenic Systemic Fibrosis in Patients With Stage 4 or 5 Chronic Kidney Disease Receiving a Group II Gadolinium-Based Contrast Agent: A Systematic Review and Meta-analysis. JAMA Intern Med 2020;180(2):223–230.
54. Fananapazir G, Bashir MR, Corwin MT, Lamba R, Vu CT, Troppmann C. Comparison of ferumoxytol-enhanced MRA with conventional angiography for assessment of severity of transplant renal artery stenosis. J Magn Reson Imaging 2017;45(3):779–785.
55. Corwin MT, Fananapazir G, Chaudhari AJ. MR Angiography of Renal Transplant Vasculature with Ferumoxytol: Comparison of High-Resolution Steady-State and First-Pass Acquisitions. Acad Radiol 2016;23(3):368–373.
56. Shahrouki P, Moriarty JM, Khan SN, et al. High resolution, 3-dimensional Ferumoxytol-enhanced cardiovascular magnetic resonance venography in central venous occlusion. J Cardiovasc Magn Reson 2019;21(1):17.
57. Lehrman ED, Plotnik AN, Hope T, Saloner D. Ferumoxytol-enhanced MRI in the peripheral vasculature. Clin Radiol 2019;74(1):37–50.
58. Hope MD, Hope TA, Zhu C, et al. Vascular imaging with ferumoxytol as a contrast agent. AJR Am J Roentgenol 2015;205(3):W366–W373.
59. Collins JD. MR Imaging of the Mesenteric Vasculature. Radiol Clin North Am 2020;58(4):797–813.